Structural Engineering and Mechanics, Vol. 18, No. 4 (2004) 475-491
DOI: http://dx.doi.org/10.12989/sem.2004.18.4.475

Numerical study of mono-strand anchorage mechanism under service load

D. Marceau†

Department of Applied Sciences, University of Quebec at Chicoutimi, Quebec, Canada, G7H 2B1

M. Fafard† and J. Bastien†

Department of Civil Engineering, Laval University, Quebec, Canada, G1K 7P4

(Received September 2001, Accepted February 2004)

Abstract. Anchorage devices play an important role in post-tensioned bridge structures since they must sustain heavy loads in order to permit the transfer of the prestressing force to the structure. In external prestressing, the situation is even more critical since the anchorage mechanisms, with the deviators, are the only links between the structure and the tendons throughout the service life of the structure. The behaviour of anchorage devise may be studied by using the finite element method. To do so, each component of the anchorage must be adequately represented in order to approximate the anchor mechanism as accurately as possible. In particular, the modelling of the jaw/tendon device may be carried out using the real geometry of these two components with an appropriate constitutive contact law or by replacing these components by a single equivalent. This paper presents the numerical study of a mono-strand anchorage device. The results of a comparison between two different representations of the jaw/tendon device, either as two distinct components or as a single equivalent, will be examined. In the double-component setup, the influence of the wedge configuration composing the jaw, and the influence of lubrication of the anchor, will be assessed.

Key words: anchorage device; contact; finite element; jaw/tendon device; lubrication; yielding; stress and strain distribution; wedge penetration.

1. Introduction

Post-tensioning is a commonly used technique in the construction industry either for new structures or to reinforce existing ones. In bridge design, post-tensioning regained popularity during the 80's with the introduction of new high performance concrete and the evolution of the post-tensioning technique itself (material, methodology,...). This technique requires the tensioning of prestressing tendons which are anchored to the concrete section using metallic anchorage devices. Different types of the device of specific shapes and mechanical characteristics may be found in the market. These are developed mainly by private companies involved in the prestressing industry and are offered in a variety of capacities, according to the size and number of tendons to be anchored.

† Professor

In this paper, the numerical behavior of a mono-strand anchorage device will be examined. In particular, the influence of the anchor gripping action will be assessed.

The design and development of anchorage mechanisms is generally carried out by companies specialized in the prestressing field using laboratory tests, and more recently, finite element analysis (Bastien *et al.* 2002). To date, very few papers have been published involving the numerical analysis of anchoring mechanisms. In this regard, Marceau (2001) and Bastien *et al.* (2002) represent one of the few papers dealing with the numerical behavior of multi-strand anchorage mechanisms.

The finite element method figures as a complementary step only to laboratory tests because these tests, while well adapted to inform about the global behaviour of the mechanism, cannot assess the state of stress/strain developed in the core of mechanism parts. It should be made clear here that a typical anchorage consists of a thick metallic cylindrical plate called the anchor head, which is perforated by one or more conical cavities in which a tendon is gripped by a jaw. This jaw is made according to the requirements of the specific post-tensioning system used, by two or three wedges called herein split-wedges. The anchor head is set on the concrete section by means of another plate called "anchor plate", the latter being bolted to the concrete.

In order to ensure adequate behaviour representation, the interaction between the components of the mechanism, as well as their non-linear behaviour, must be take into account for in a finite element model. Therefore, a proper model should take into consideration the modelisation of : solids using an elasto-plastic law and a large strain approach, contact between the anchor head and anchor plate interface, contact between each jaw and the corresponding anchor head conical cavity and contact between the jaw and the gripped tendon.

Marceau *et al.* (2002) and Marceau *et al.* (2001b) describe the numerical model that will be used from now in the text, as well as the description of the different anchor components and the associated contact interfaces. More over, the authors introduce a new constitutive contact law called the gripping/contact law based on a phenomenological approach to simulate the jaw gripping action on a tendon. Identification of the law parameters was done using the finite element method in combination with a neural network approach and results of experimental tests conducted on five mono-strand anchorage devices. This gripping/contact law will be used in this paper to study the behaviour of a mono-strand anchor head in relation with the uniformity of the gripping action. Figs. 1 to 3 give geometric details of a jaw made of three metallic pieces assembled together (split-wedges) at the top using a metallic ring. The finite element analysis which have been conducted to date were all implicitly based on the fact that the spilt-wedges were uniformly distributed around the tendon

Fig. 1 Mono-strand anchorage

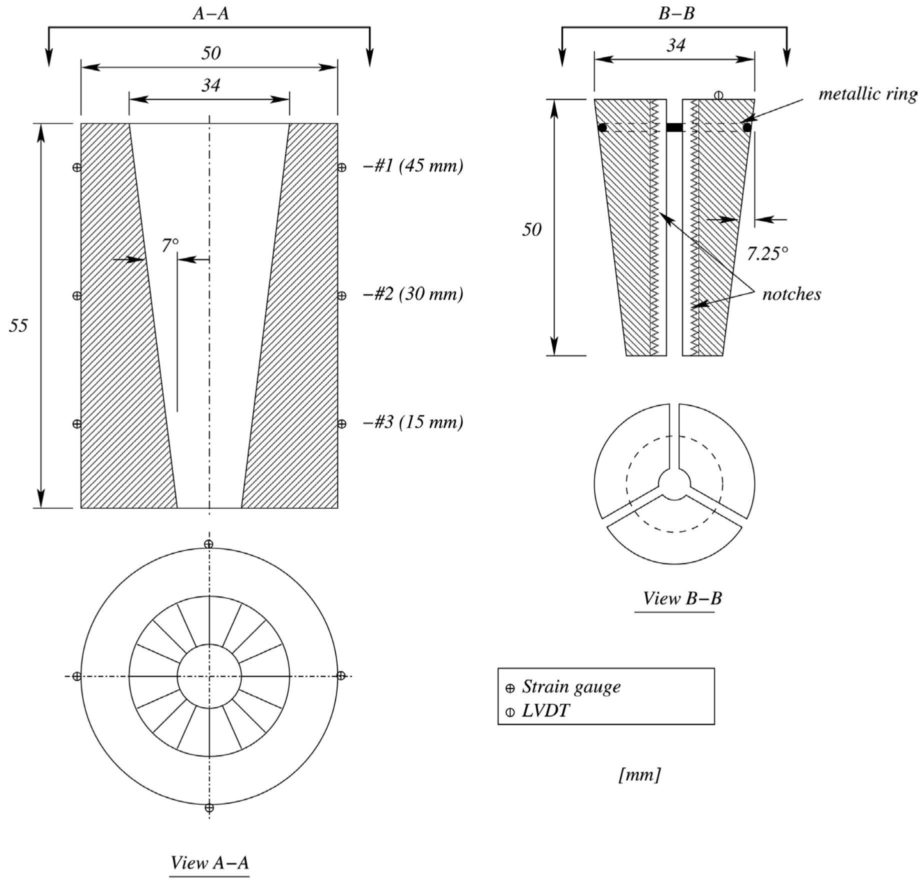

Fig. 2 Geometrical description of the anchorage device

and installed as such during construction, as shown in Fig. 4 for case 1. However, due to construction practice, this condition represents an ideal situation, and wedge regrouping, such as described in cases 2 and 3 of Fig. 4 are possible; case 3 being considered as the extreme situation.

Therefore, the aim of this paper is to describe the influence of different split-wedges and will include configurations of mono-strand anchor head behaviour. Three different cases are examined and numerical information regarding the von Mises equivalent stress distribution in the anchor head, as well as at the surface periphery of the anchor head are presented. The penetration of the split-wedges along the anchor head conical cavity is also presented under service loading. In order to assess another extreme case in connection with the penetration of the jaw along the anchor cavity, the practice of lubrication will be examined. Finally, the paper will provide additional information related to the way the jaw-tendon assembly is represented in the numerical model.

The jaw and tendon may be represented as two different components or by a single equivalent system. In the latter representation, the jaw/tendon gripping action is considered to be such that the two components (jaw and tendon) are assumed to act as a unit. Therefore, the jaw/tendon assembly is replaced by a single truncated conical component. This component has the same global dimensions as the jaw/tendon assembly, and is meshed as such. Since, in practice, the wedges are

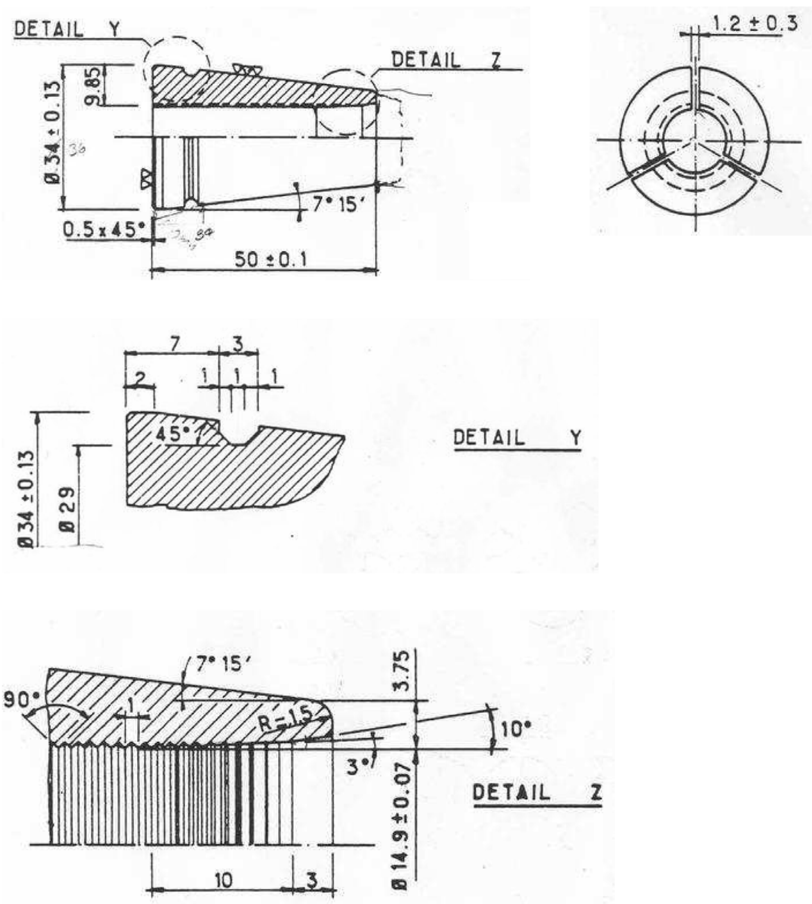

CEMENTING AND HARDNESS
Cementing depth: 0,3 to 0,5 mm
Hardness of the cemented layer: 60 to 65 HRc
Internal hardness: 20 to 25 HRc

Drawn from: COMMISION INTERMINISTÉRIELLE DE LA PRÉCONTRAINTE

Fig. 3 Details of the wedge gripping devices

thick pieces submitted to a surface hardening process, and since a tendon exhibits linear elastic behaviour under service loads, the cone associated to the device is considered to be linear elastic. For this jaw-tendon representation, the load is applied at the top of the truncated cone by imposing a uniform pressure on the equivalent jaw/tendon system. In the case where the jaw and tendon are considered as two different components, loading is applied by pulling the bottom end of the tendon.

2. Numerical model

The complexity of the mechanical behaviour of an anchorage device provides a broad range of investigative possibilities. During the process of submitting the anchorage device to heavy prestressing loads, a number of phenomena may be observed including : wedge-tendon gripping

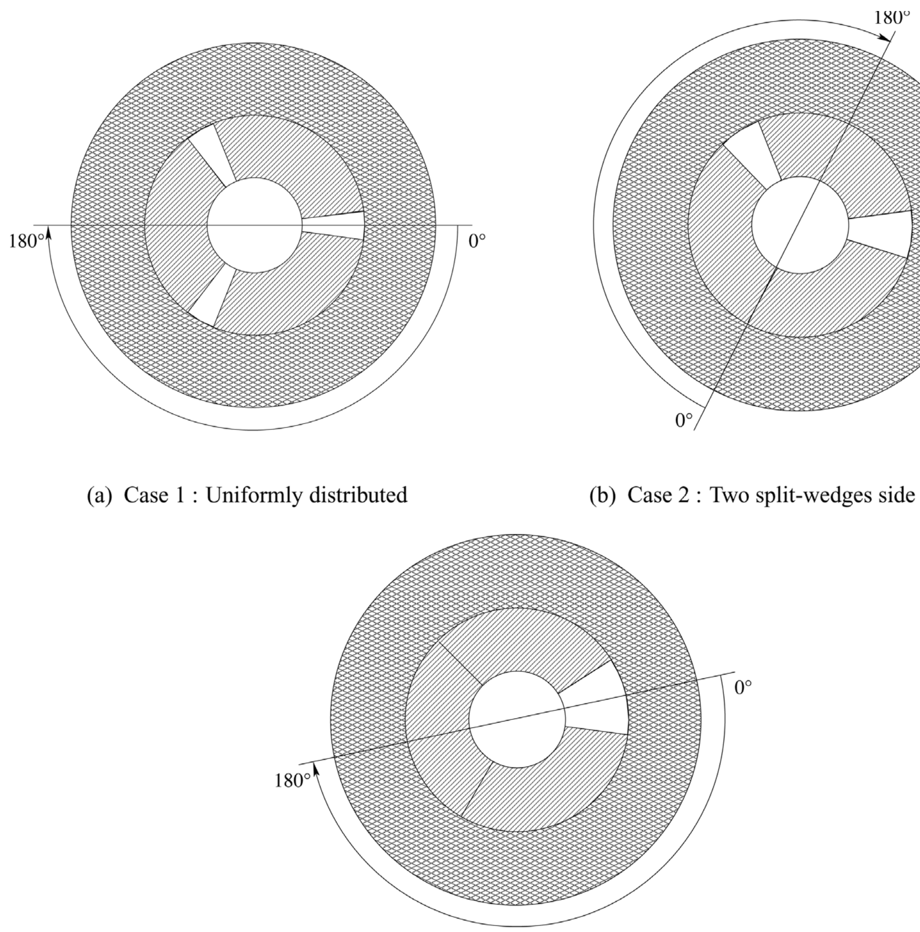

(a) Case 1 : Uniformly distributed

(b) Case 2 : Two split-wedges side by side

(c) Case 3 : Three split-wedges side by side

Fig. 4 Details of the split-wedge configurations

action; friction at the wedge/cavity interfaces; friction at anchor block/anchor plate interface; plastic strains; and large relative displacements at certain interfaces. An adequate finite element model should be able to take into account all these mechanical phenomena.

This study, takes in to account three types of nonlinearity : large strain (large displacement), plasticity, and contact between certain interfaces. In the latter, large relative displacement between interfaces has been considered using a slave-master concept (Marceau 2001, Laursen and Simo 1993). The penalty/augmented Lagrangian method has been used for the evaluation of the stresses at the various interfaces. This approach yields accurate results and makes non-compatible meshes possible between different components of the anchorage device. All mathematical and numerical techniques used for this model can be found in Marceau (2001). The model has been tested and validated using information from the literature.

It should be noted in, that for the wedge-tendon contact interface (see Fig. 3), a new contact law taking into account all the experimental observations is necessary (Marceau *et al.* 2002). Firstly, the

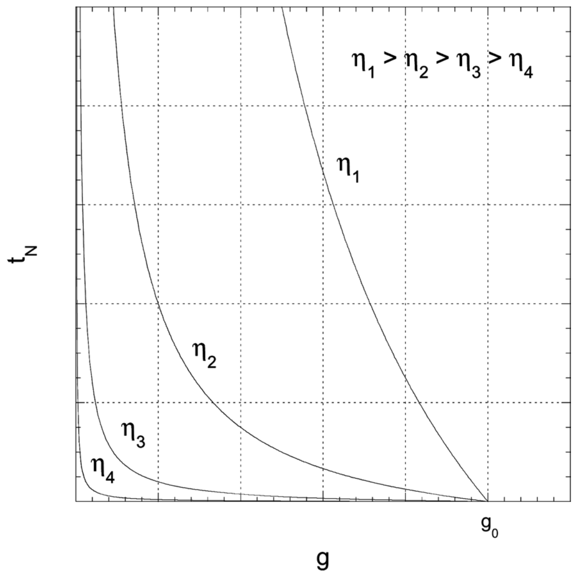

Fig. 5 Normal stress law for the wedge-tendon interface

interface behaviour is considered orthotropic in the RTL directions. The normal contact stresses are assumed to act in the radial direction (R), while the longitudinal direction (L) is considered parallel to the tendon profile. While a Coulomb friction law is considered in the tangential direction (T), no relative displacement is assumed between the tendon and wedges in the longitudinal direction (L). Indeed, in this direction, and contrary to the wedge-alveolus interface, the relative displacement is considered very small, allowing for the present simplification. In the radial direction, hyperbolic law is proposed and defined as (see Fig. 5):

$$t_R = \frac{\eta g_u}{g} \tag{1}$$

where η represents the stiffness in the radial direction and g, the actual radial distance between the wedge and the tendon, such that:

$$g = g_0 - g_u \tag{2}$$

$$g_u = -\underset{\sim}{n} \cdot [\underset{\sim}{u}^1(\underset{\sim}{X}^1, t) - \underset{\sim}{u}^2(\underset{\sim}{\Psi}_0(\bar{\underset{\sim}{\xi}}), t)] \tag{3}$$

where g_0 defines the fictitious gap between the wedge and the tendon. The terms $\underset{\sim}{u}^1$ and $\underset{\sim}{u}^2$ represent the displacement field of the slave and master contact surfaces respectively.

The parameter g_0 can be associated with the depth of the notches. As seen in Fig. 5, for a given η value, when $g = g_0$ the radial stress is zero. At this point, the notches begin to penetrate into the tendon and the stiffness increases progressively. When $g_u \to g_0$, the latter being the maximum allowed penetration, the radial stress increases rapidly. This radial stress will increase more or less rapidly depending on the value of η. Thus η and g_0 can be considered as unknown parameters that need to be identified.

From a mathematical point of view, the admissible conditions can be defined by:

$$\left.\begin{array}{c} g \geq 0 \\ g \leq g_0 \\ t_R \geq 0 \\ t_R(\underset{\sim}{X}^1, t)g(\underset{\sim}{X}^1, t) \geq 0 \end{array}\right\} \tag{4}$$

For the radial direction and

$$\left.\begin{array}{c} \Phi = \left\|t_{T_T}\right\| - \mu_{wt}t_R \leq 0 \\ \dot{\xi}^T - \zeta\dfrac{t_{T_T}}{\left\|t_{T_T}\right\|} = \dfrac{1}{\varepsilon_T}\dot{t}_{T_T} \\ \dot{\xi}^L = \dfrac{1}{\varepsilon_L}\dot{t}_{T_L} \\ \zeta \geq 0 \\ \Phi\zeta = 0 \end{array}\right\} \tag{5}$$

for the longitudinal and tangential directions with μ_{wt}, $\dot{\xi}^L$ and $\dot{\xi}^T$, defining the Coulomb friction coefficient in the tangential direction and the wedge-tendon relative velocities in the corresponding directions. In the same manner, $\dot{t}_{T_L}$ and $\dot{t}_{T_T}$ represent the stress rate along the longitudinal and tangential directions respectively. Regularization is obtained using the penalty numbers ε_L and ε_T.

3. Finite element simulation

Taking into consideration the geometrical symmetry of the mono-strand anchorage device, only one-sixth of it has been represented when the split-wedges where considered uniformly distributed around the tendon, as in case 1 (see Fig. 4(a)). When two or more split-wedges are grouped around the tendon, as for cases 2 and 3, one-half of the anchorage device has been modelled (Fig. 4(b) and Fig. 4(c)). The different meshes are presented in Fig. 6. For these meshes, symmetry conditions have been applied in a standard way, while quadratic interpolation elements were used to discretize the various anchorage components. These hexahedral and triangular prism elements were based on the large strain deformation theory, and $3 \times 3 \times 3$ Gauss points and 3×3 Hammer-Gauss points were the schemes used respectively for integration. For the contact interfaces, eight-noded quadrilateral and six-noded triangular elements were used. Their integration schemes were based on a 3×3 Gauss points and a three Hammer points respectively. The numerical resolution was performed using the Newton-Raphson and arc-length methods. Contact interfaces were solved using a penalty coefficient of 10^5 in both normal and tangential directions, using four Lagrangian augmentations.

Since each split-wedge occupies a conical portion of 112^o inside the anchor cavity, in the ideal case of their proper distribution inside this cavity, each split-wedge will be separated from the two others at an angle of 8^o. This angle corresponds to an arc length of about 2.4 mm at the top portion

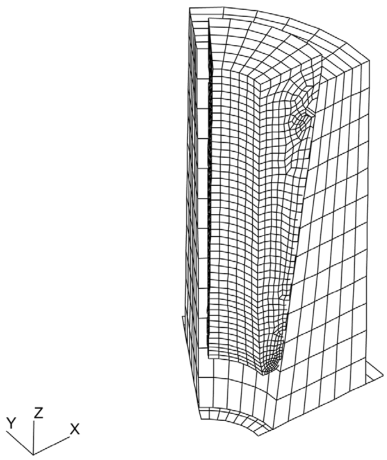

(a) Case 1: split wedges

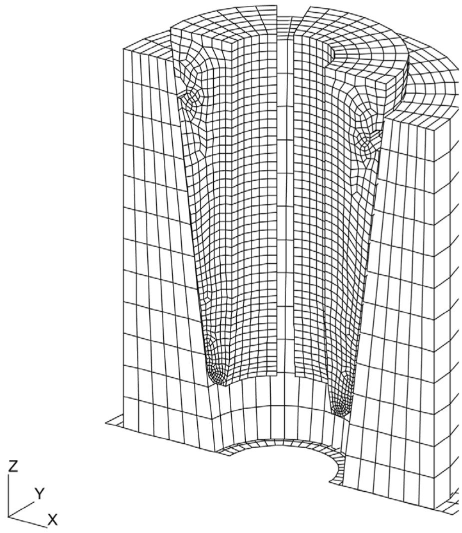

(b) Case 2

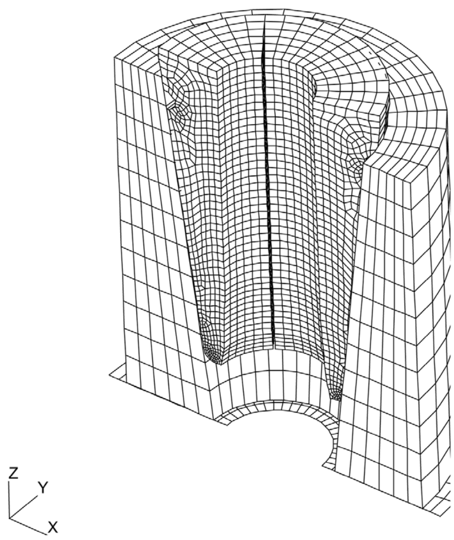

(c) Case 3

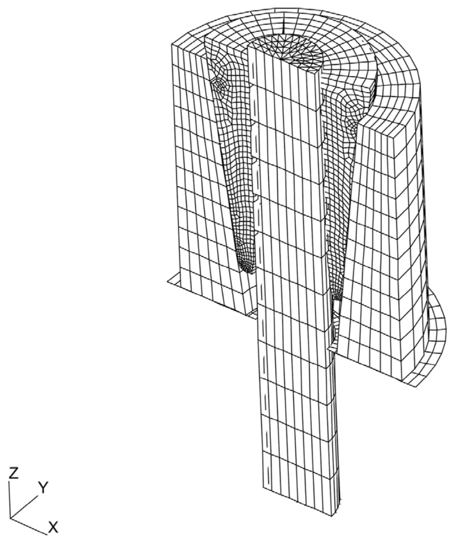

(d) Full mesh (case 3)

Fig. 6 Mesh of the anchorage device for each case

of the anchor cavity perimeter. Fig. 6(a) shows one-sixth of the discretized anchorage device, which incorporates one-half wedge (sector of 56^{o}). Therefore, a free space, corresponding to an angle of 4^{o}, is apparent in Fig. 6(a). Along the two symmetric axes shown, usual symmetric conditions were applied leaving one side of the wedge portion represented in Fig. 6(a) free from any boundary conditions. It is also obvious in this figure that the jaw/tendon system exceeds the top of the anchor head by 5.0 mm before loading, as observed in laboratory during testing. The anchor head was considered to set on a rigid support in order to represent the experimental setup. The finite element mesh associated with Fig. 6(a) is made up 3,828 elements, 4,057 nodes, and 12,171 degrees of freedom.

As shown in Fig. 4(b), case 2 deals with the situation where two of the three wedges grouped side by side, leaving two free portions of about 3.6 mm in arc length. For case 3, the three wedges are side by side, leaving only one 7.2 mm arc length opening (see Fig. 4(c)). In these two situations, one-half of the anchorage device (sector of 180^o) has been discretized. As shown in Figs. 6(b) and 6(c), these meshes incorporate one entire wedge (sector of 112^o) plus one-half wedge (sector of 56^o). In these two situations, some additional contact interfaces arise from the wedge regrouping. Indeed, one and two additional contact interfaces must be taken into account at the joining wedges for cases 2 and 3 respectively. As can be seen in Fig. 6(c), a small gap still exists and appears at one of two additional interfaces. This situation results from the complex geometry of the wedges, as shown already in Fig. 3. In cases 2 and 3, 11,890 elements and 11,447 nodes constitute the meshing leading to a total of 34,341 degrees of freedom for case 2 and 34,206 degrees of freedom for case 3.

Tables 1 and 2 show the anchor components and tendon mechanical characteristics used in the numerical analysis. The anchor head exhibits an elasto-plastic behaviour while the split-wedges are considered elastic, due to the high hardness of their surface corresponding to a heat treatment process (Bastien 1992).

Consideration of contact is based on the work of Marceau (2001). The Coulomb frictional coefficient between the anchor head and anchor plate (μ_{hp}) were set to 0.3 while the one between the jaw and anchor cavity (μ_{hw}) was fixed to 0.09. As far as the gripping/contact law is concerned, the following parameters were used: the stiffness parameter was set to η = 3,000 MPa, the Coulomb frictional coefficient in the tangential direction to μ_{wt} = 0.3 and the maximum gripping depth to g_0 = 1.5 mm as described in Marceau *et al.* (2002).

Table 1 Mechanical properties of the anchorage device

Component	Yield limit (MPa)	Ultimate stress (MPa)	Strain at failure (%)
Anchor head	400	750	16
Anchor plate	260	400	22
Wedge	400	Elastic behaviour	
Young modulus: 2,0 $\cdot$ 10^5 MPa, Poisson ratio: 0,30			

Table 2 Characteristics of the tendon

Effective area (mm^2)	139
Nominal stress at failure (MPa)	1770
Nominal force at failure (kN)	246
Admissible stress (MPa) (0,8 $\cdot$ 1770)	1416
Admissible stress (kN)	197
Young modulus: 2,0 $\cdot$10^5 MPa, Poisson ratio: 0,30	

4. Results and discussion

As prescribed by many design codes (Bastien *et al.* 2002), the admissible service load corresponds to 80 percent of the ultimate strength of the tendon ($0.80F_u$). This load level represents the maximum prestressing force allowed during jacking procedure. Considering the characteristics of the tendon described in Table 2, all finite element results are presented for a maximum load of 196 kN, corresponding to $0.80F_u$. The first part of this section deals with the influence of the jaw/tendon device on the behaviour of the anchorage mechanism. Secondly, some results are presented with regard to the influence of the split-wedges configuration (cases 1 to 3) and finally, the numerical model is used to simulate the effect of lubrication of the jaw/cavity interface.

4.1 Jaw/tendon device versus truncated cone

Fig. 7 shows the influence of the real jaw/tendon device on the behaviour of the anchorage mechanism, comparatively to a monolithic truncated cone for the numerical simulation of anchorage mechanisms, as performed by Marceau *et al.* (2001a). In the former, three dimensional analysis were performed using the mesh shown in Fig. 6(a). For the latter, the particular symmetry condition implies the possibility to solve the problem using axisymmetrical formulation. To provide a valid comparison, both models were studied using the same Coulomb frictional coefficient (0.09) between the jaw and the cavity. Firstly, Fig. 7(a) shows that the penetration of the jaw/tendon device is larger than that occurring with the truncated cone (3.3 mm versus 0.4 mm at ($0.80F_u$)). The small penetration of the cone is due to its large stiffness in the radial and circumferential directions. In this sense, it is clear that the truncated cone allows lower values of stress and strain that those

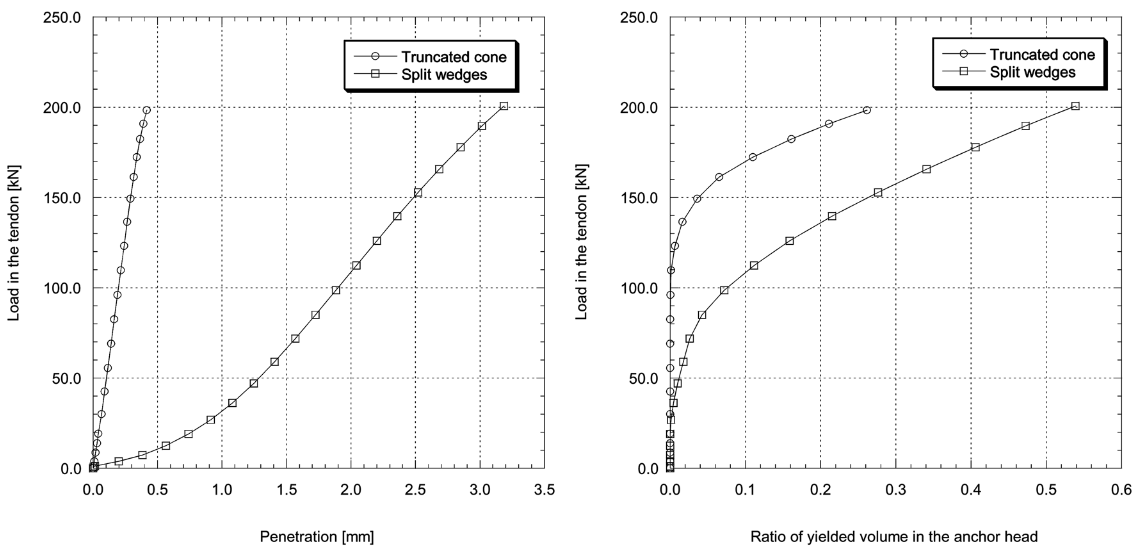

(a) Penetration of the gripping device into the cavity (b) Yielding of the anchorage

Fig. 7 Influence of the split-wedges on the behaviour of the anchorage device obtained with the jaw/tendon device. For the jaw/tendon device, the gripping/contact constitutive law, as well as the gap between wedges, allow progressive penetration of the triangular notches in the tendon. It should be noted that similar values for the penetration of the jaw/tendon device in the cavity were obtained from experimental tests (Marceau *et al.* 2002). This penetration of the jaw/tendon device causes an increase of the yielded volume of the anchorage head, as shown in Fig. 7(b), comparatively to the truncated cone. Considering these facts, it can be hazardous to draw practical conclusions from the numerical simulations or tests using truncated cones.

4.2 Misalignment of the wedges in the cavity

In this sub-section, numerical simulations were performed to study the influence of splitwedge misalignment on the mechanical behaviour of the anchorage mechanism. The three most critical split-wedge configurations are described in Fig. 4, and defined as cases 1 to 3 respectively. As

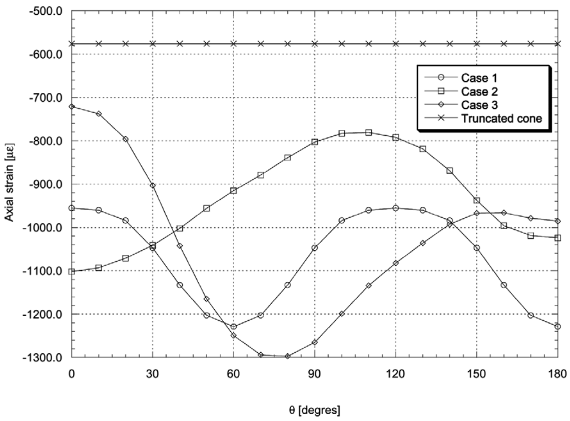

(a) Level: 15mm

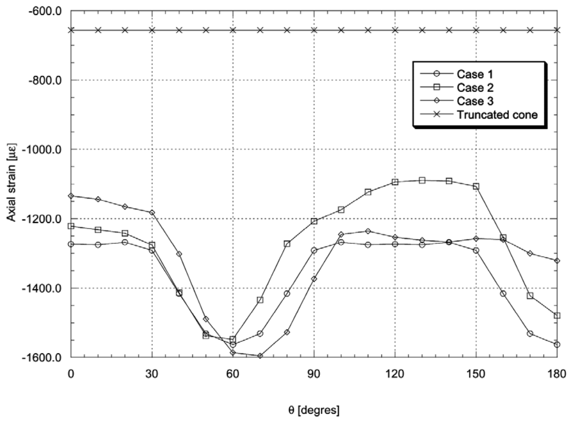

(b) Level: 30mm

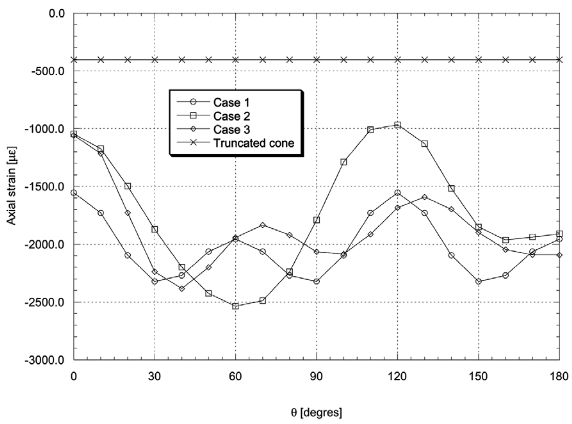

(c) Level: 45mm

Fig. 8 Axial strain for three levels along peripheral face of the anchor block

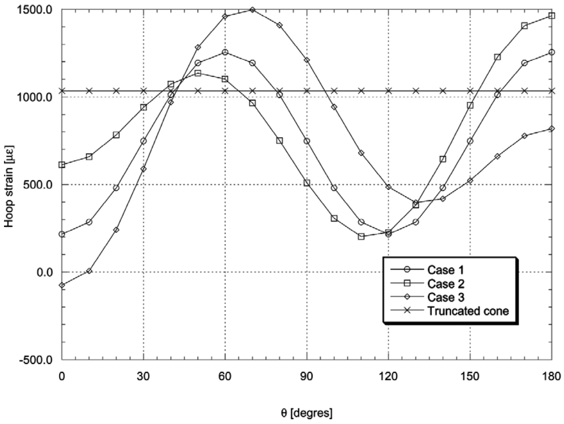

(a) Level: 15mm

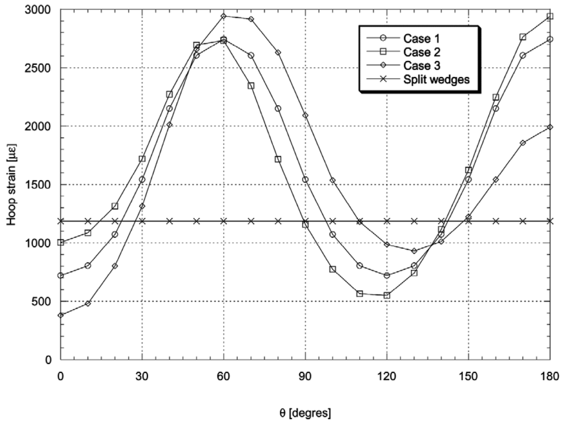

(b) Level: 30mm

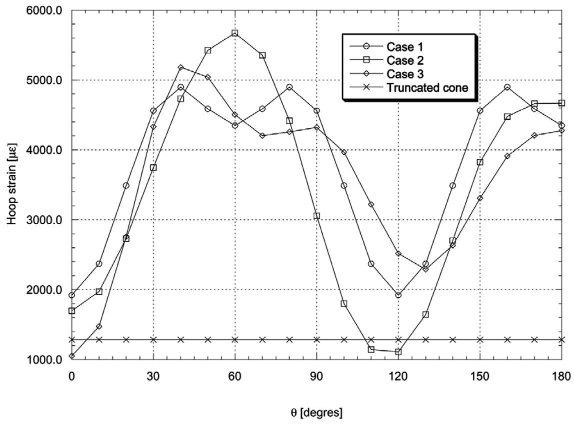

(c) Level: 45mm

Fig. 9 Hoop strain for three levels along peripheral face of the anchor block

described in Fig. 2, the total height of the anchor block is 55 mm. Figs. 8 to 10 show the strain distribution on the peripheral face of the anchorage head at three different levels: 15, 30, and 45 mm from base. Referring to Fig. 4 for the definition of the angle (θ), these last figures show that there is a large difference between strains obtained with the split-wedge and the truncated cone, which is a constant value. In particular, it is shown that strains increase for angles corresponding to the middle of a wedge and, therefore, to the location between the wedge and the anchor block where pressure value is maximum. In this manner, the strain values are higher at the top of the anchor block and decrease to the bottom. Also, Fig. 10 shows that radial strain distribution causes the anchor block to deform according to an elliptic shape. This situation has the effect of reducing the total contact area between the tendon/wedge device and the cavity and, therefore, the efficiency of the anchor block.

On the other hand, the Fig. 11 shows the von Mises stress distribution along the same paths. It can be concluded that the misalignment of the split-wedge does not affect the results significantly.

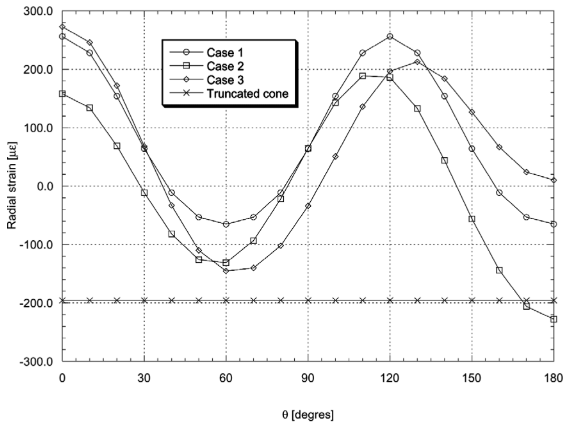

(a) Level: 15mm

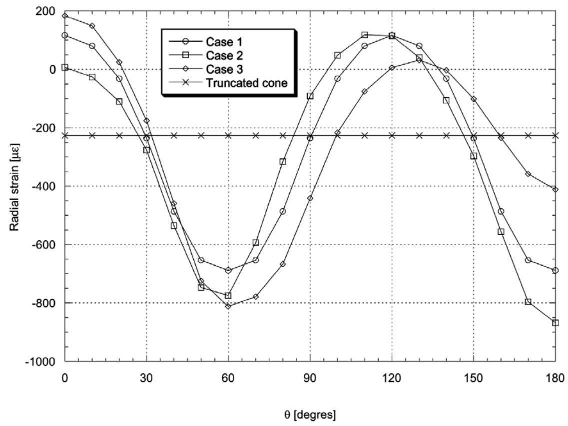

(b) Level: 30mm

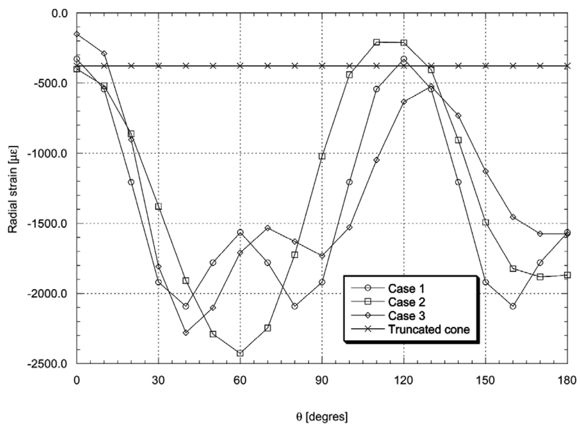

(c) Level: 45mm

Fig. 10 Radial strain for three levels along peripheral face of the anchor block

However, the use of the real jaw/tendon provides the possibility to identify yielded regions for which the truncated cone has never reached the yield stress. Also, Fig. 11 shows that von Mises stress increases from the region located between two wedges (θ = 0^o, 100^o) to a maximum value located near to the middle of a wedge (θ = 60^o, 180^o). Along the height of the anchor block, yielding appears from the top (45 mm) and spreads over the second level (30 mm), but not over the level corresponding to 15 mm. Compared to the results obtained with the jaw/tendon device, it can be concluded that those of the truncated cone are largely underestimated.

Finally, Fig. 12 shows that the misalignment of the split-wedge has no significant effect on the penetration of the jaw/tendon device in the cavity or on the yielded volume. However, this is not the case if these results are compared with those obtained with the truncated cone (see Fig. 7) for which the difference is very significant.

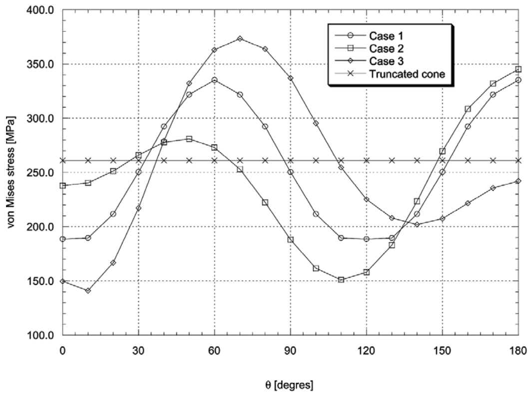

(a) Level: 15mm

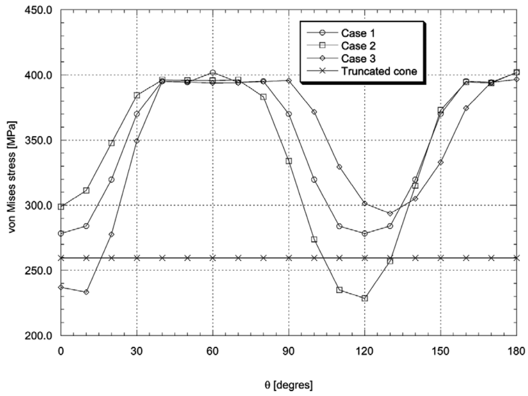

(b) Level: 30mm

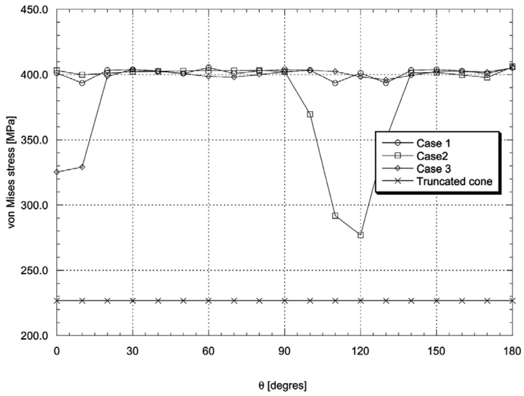

(c) Level: 45mm

Fig. 11 von Mises stress for three levels along peripheral face of the anchor block

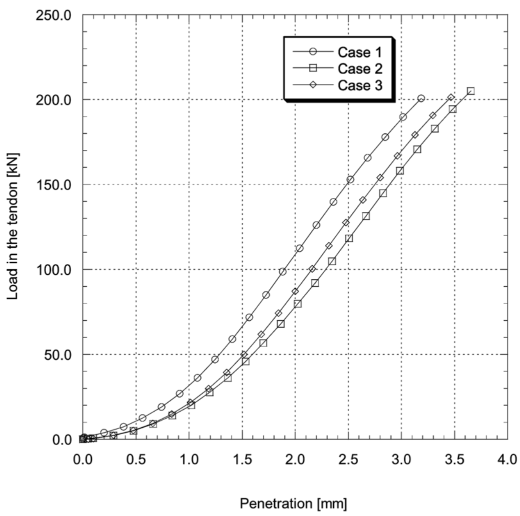

(a) Penetration of the jaw/tendon device into the cavity

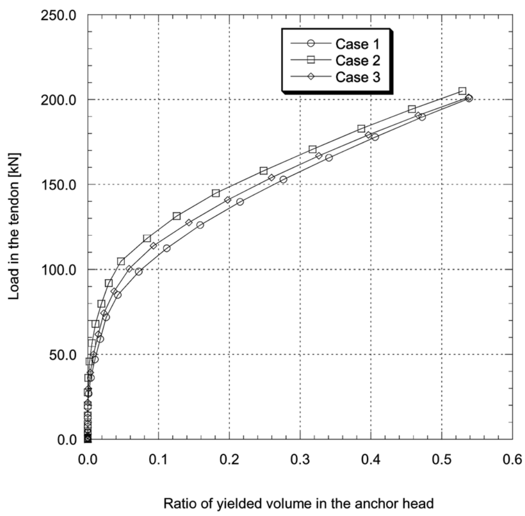

(b) Yielding of the anchorage

Fig. 12 Influence of the split-wedge configuration on the behaviour of the anchorage device

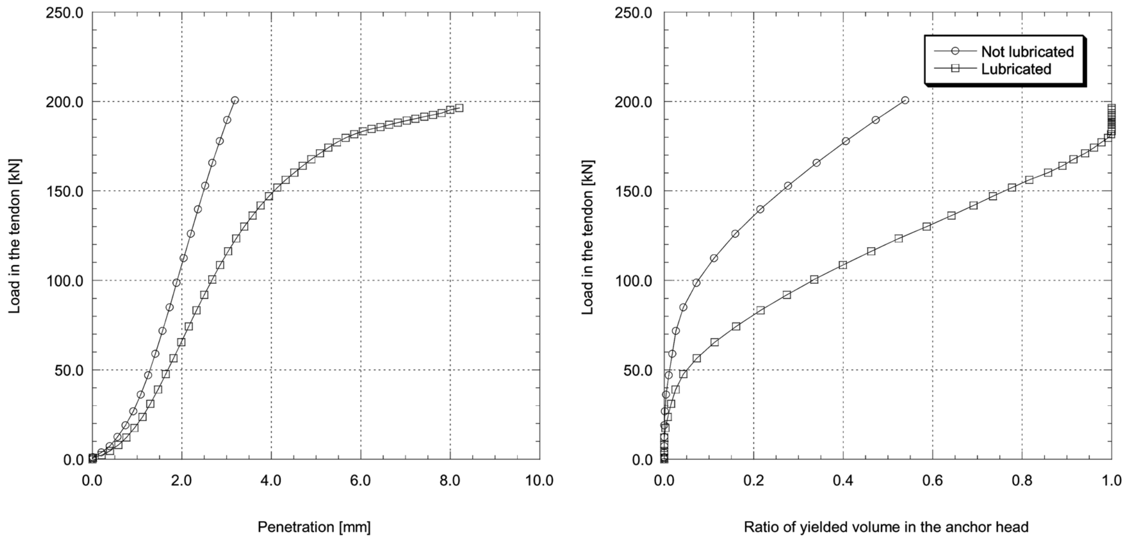

(a) Penetration of the jaw/tendon device part into the cavity (b) Yielding of the anchorage

Fig. 13 Influence of lubrication on the behaviour of the anchorage device

4.3 Lubrication of the jaw/cavity interface

The lubrication of the jaw/cavity interface can be studied by reducing the Coulomb frictional coefficient at this interface. To do so, the value is modified from 0.09 to 0.02, which can be compared to a lubrication using graphite paste. Using the ideal split-wedge configuration (see Fig. 4), Fig. 13 shows that lubrication has a significant effect on the penetration of the jaw/tendon device and the yielded volume. Particularly, Fig. 13(b) shows that the whole volume of the anchor bloc is

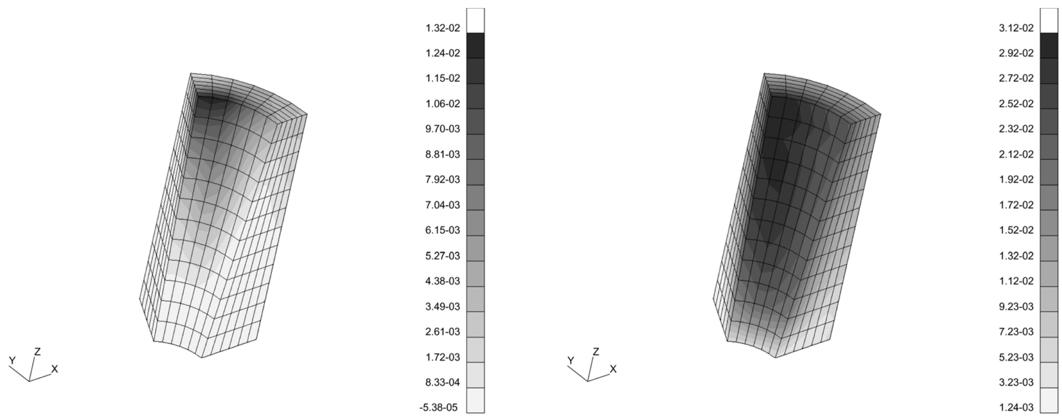

(a) Non-lubricated case (b) Lubricated case

Fig. 14 Influence of lubrication on the equivalent plastic strain distribution yielded for the lubricated case. In the same way, Fig. 14(b) indicates that the equivalent plastic strain increases by about 130 percent for the lubricated case, compared with the case without lubrication, which is in agreement with the excessive penetration of the wedges as shown in Fig. 13(a).

5. Conclusions

In this paper, a comparative finite element study was presented to verify the influence of the jaw/tendon device on the mechanical behaviour of an anchorage mechanism. To do so, simulations were performed using a truncated cone, which can be seen as an idealization of the real jaw/tendon device, and finally, with the real jaw/tendon device itself. The latter was modelled using particular contact constitutive law at the jaw/tendon interface to adequately simulate the penetration of the triangular notched into the tendon. The results show that such modelling provides a better way to represent the real behaviour of the anchorage mechanism which has been confirmed by experimental tests. In particular, the use of the jaw/tendon device has a significant effect on the yielding of the anchor block, due to the excessive penetration of the jaw/tendon device into the alveolus. This situation is mainly due to the gap between each wedge composing the jaw, providing the possibility for each of them to be easily deformed along hoop and radial directions.

Also, simulations were carried out to verify the effect of misalignment of the split wedges composing the jaw. The considered cases show that misalignment has no significant effect on the penetration of the jaw/tendon device and yielding of the anchor block. However, the results presenting strains and von Mises stress distributions demonstrate that the higher values are located in the regions where contact pressures are maximum, such as in the middle of a wedge.

Finally, some results are presented regarding the effect of lubrication of the jaw/alveolus interface. This procedure, which is very widespread in practice, is very faithful and is not recommended due to the effect of the excessive penetration of the jaw/tendon device in the anchor block, and of course, the high yielding level reached in the anchor block.

Acknowledgements

The authors would like to gratefully acknowledge the collaboration of Mr. Jean-Xavier Gartner, engineering student at the catholic school for the Arts and Crafts, France (Ecole Catholique des Arts et Métiers, France). Partial support of this research by the Quebec Ministry of Transportation, the Natural Sciences and Engineering Research Council of Canada, and the Quebec Funding for Research in to Nature and Technology (Fonds québécois de la recherche sur la nature et les technologies), is also gratefully acknowledged.

References

Bastien, J. (1992), “Comportement des têtes d’ancrage mono et multi-torons: Étude expérimentale et étude par éléments finis”, Ph.D. thesis, Département de génie civil, Université Laval, Québec.

Bastien, J., Marceau, D., Fafard, M. and Ganz, H. (2002), “Mechanical behaviour of multistrand anchorage mechanisms under service and ultimate loads”, *J. Bridge Eng.*, ASCE, Submitted.

Laursen, T.A. and Simo, J.C. (1993), "A continuum-based finite element formulation for the implicit solution of multibody, large deformation frictional contact problem", *Int. J. Num. Meth. Engng*., **36**, 3451-3485.

Marceau, D. (2001), "Modélisation du contact tridimensionnel en grands déplacements relatifs et son application à l'étude des dispositifs d'ancrages multitorons", Ph.D. thesis, Département de génie civil, Université Laval, Qu´ebec.

Marceau, D., Bastien, J., Fafard, M. and Chabert, A. (2001a), "Experimental and numerical studies of mono-strand anchorage", *Int. J. Struct. Eng. Mech.*, **12**(2), 119-134.

Marceau, D., Fafard, M. and Bastien, J. (2002), "Constitutive law for wedge-tendon gripping interface in anchorage device – Numerical modeling and parameters identification", *Int. J. Struct. Eng. Mech.*, **15**(6), 609-628.

Marceau, D., Fafard, M., Bastien, J. and Boudjelal, M. (2001b), "Application des réseaux neuromimétiques à la détermination du comportement déformationnel d'un dispositif d'ancrage multitorons", In "Actes du cinquième colloque en calcul des structures", **1**, 189-196. Ed. Batoz, Ben Dhi & Chauchot (Tecknea, Toulouse), Giens, France.

SC